

On the optimum performance-based design of eccentrically braced frames

Reza Karami Mohammadi* and Amir Hossein Sharghi^a

Civil Engineering Department, K.N. Toosi University of Technology (KNTU), Tehran, Iran

(Received January 13, 2013, Revised August 20, 2013, Accepted November 15, 2013)

Abstract. The design basis is being shifted from strength to deformation in modern performance-based design codes. This paper presents a practical method for optimization of eccentrically braced steel frames, based on the concept of uniform deformation theory (UDT). This is done by gradually shifting inefficient material from strong parts of the structure to the weak areas until a state of uniform deformation is achieved. In the first part of this paper, UDT is implemented on 3, 5 and 10 story eccentrically braced frames (EBF) subjected to 12 earthquake records representing the design spectrum of ASCE/SEI 7-10. Subsequently, the optimum strength-distribution patterns corresponding to these excitations are determined, and compared with four other loading patterns. Since the optimized frames have uniform distribution of deformation, they undergo less damage in comparison with code-based designed structures while having minimum structural weight. For further investigation, the 10 story EBF is redesigned using four different loading patterns and subjected to 12 earthquake excitations. Then a comparison is made between link rotations of each model and those belonging to the optimized one which revealed that the optimized EBF behaves generally better than those designed by other loading patterns. Finally, efficiency of each loading pattern is evaluated and the best one is determined.

Keywords: performance-based design; structural optimization; uniform deformation theory; seismic loading pattern; eccentrically braced frame; nonlinear dynamic analysis

1. Introduction

Currently, seismic design provisions of most building codes are based on strength or force (base shear) considerations. These building codes are generally regarding the seismic effects as equivalent static forces with a height wise distribution which is consistent with the first vibration mode shape. However, it should be noticed that during strong earthquakes the structure enters its inelastic range of behaviour and its vibration characteristics change significantly. As it was expected, current studies indicate that these design procedures will not necessarily result in a desirable response of structure in the selected performance level (Anderson *et al.* 1991, Hart 2000, Martinelli *et al.* 2000, Moghadam and Hajirasouliha 2006a). As an example, Chopra (2001) evaluated the ductility demands of several shear building models subjected to the El-Centro Earthquake and concluded that the use of distribution patterns of the earthquake forces specified in

*Corresponding author, Assistant Professor, E-mail: address: rkarami@kntu.ac.ir

^a M.Sc. Student, E-mail: asharghi@mail.kntu.ac.ir

the Uniform Building Code (UBC 1997) does not lead to equal ductility demand in all stories, and that in most cases the ductility demand in the first story is the largest of all stories. In another research, Lee and Goel (2001) analyzed a series of 2 to 20 story one-bay frame structures subjected to various earthquakes and concluded that in general there is a significant difference between the earthquake-induced shear forces and the forces determined by assuming distribution pattern of UBC (1997), which revealed that this distribution pattern cannot be a good representation of earthquake forces.

In an attempt to optimize conventional lateral load distribution suggested by codes for seismic design, Deguchi *et al.* (2008) obtained a pattern for maximum shear response of an elastic shear bar with both uniform stiffness and mass distributions, based on the assumption that the velocity spectrum of ground motion is independent of the natural period. They used this pattern as an alternative to the distribution of seismic loads given in Japanese standard (BJC 1997) and made a comparison of these equations with regard to both leveling of the story drift angle distribution and minimization of the maximum story drift angle in all the stories of a multistory frame. Karami Mohammadi (2001), Karami Mohammadi *et al.* (2004) adopted an optimization algorithm for design of shear building models, and indicated that its application results in a uniform distribution of deformation over the height of the structure for a given seismic event. The concept behind this method is called *Uniform Deformation Theory (UDT)*. Based on this concept, they proposed a new load pattern which was a function of fundamental period and target ductility of the structure. They showed that the application of this load pattern leads to a structure with a rather more uniform inter-story ductility distribution compared to the structures designed according to UBC (1997) load pattern. Following these studies, Hajirasouliha (2005) proposed an effective optimization algorithm with an improved convergence speed in order to implement *UDT* in design of shear building models. He proposed another load pattern which was also a function of structural characteristics (i.e., fundamental period and target ductility of the structure). The most recent work in this field is that of Moghaddam *et al.* (2012), in which they have investigated the efficiency of 9 different lateral load patterns to lead to the equal ductility demands in all stories of steel moment frames. Although, none of the lateral load patterns considered in this study was able to produce the state of uniform deformation over the height of the structure, but it is shown that the load patterns which are a function of structural characteristics are more efficient than others, e.g. lateral load patterns proposed by Karami Mohammadi *et al.* (2004), Hajirasouliha (2005) and Park and Medina (2006).

In this paper, the seismic behaviour of eccentrically braced frames (EBF) is optimized by uniform distribution of shear deformation in the link-beams. This is done by iterative nonlinear dynamic analysis of 3, 5 and 10 story EBFs subjected to 12 earthquake records. Subsequently, shear strength distribution pattern and link rotations of optimized EBFs are compared to the same quantities corresponding to the structures designed according to four existing load patterns. Based on the results, application of *UDT* leads to a structure with a rather more uniform inter-story drift distribution. As a result, these structures suffer less damage as compared with structures designed for other loading patterns.

2. Optimization using uniform deformation theory

2.1 Concept of UDT

Uniform Deformation Theory (UDT) which was first proposed by Karami Mohammadi

(Karami Mohammadi 2001, Karami Mohammadi *et al.* 2004), is based on this concept that the structural weight of a lateral load resisting system with uniformly distributed ductility demand-to-capacity ratio (or any other damage index) will be minimal compared to the weight of an ordinary designed system in which deformation is not distributed uniformly and just some of structural elements have reached their ultimate states. In other words, the structural weight of a lateral load resisting system decreases as the deformation approaches to a uniform status. As a result, it can be said that an optimum distribution of material is correlated with the optimum performance of the structure during the given earthquake.

Based on this theory, inefficient material should be shifted from strong parts of the structure to the weak areas. As a consequence, the properties of structure will be updated and the modified structure will behave differently under the design earthquake. Karami Mohammadi *et al.* (2004) showed that if this alteration is applied incrementally the numerical calculations will converge to a state of uniform deformation. To meet the convergence conditions, the process of strength modification should be based on a well established algorithm. Karami Mohammadi *et al.* (2004) proposed an algorithm which in each step introduces 5% reduction in the strength of the story with the least ductility demand. The strength-deformation reciprocal relation suggests that if the strength in a part decreased, the deformation would increase. Hence, if the strength of the story with the least ductility demand is decreased incrementally, we would eventually obtain an optimal design with a state of uniform deformation.

Since in the algorithm proposed by Karami Mohammadi *et al.* (2004) only strength of one part is modified in each step, the convergence speed is slightly low and optimization process needs a high number of iterations to achieve an optimal design. In this regard, Hajirasouliha (2005) proposed an effective method for changing the component strength in each step, which increases convergence speed of the algorithm and improves the optimization process greatly. The concept of this method is to modify strength of all components in a single step. For this purpose, the modified strength assigned to each component or part of structure, S_{i+1} , can be determined based on the strength at the previous step, S_i , corresponding ductility demand, μ_i , and the target ductility demand, μ_0 , using the following equation

$$S_{i+1} = S_i \left(\frac{\mu_i}{\mu_0} \right)^\alpha \quad (1)$$

In above equation, α is the convergence coefficient which should be selected so that no significant changes occur in deformation demand of structural components. Usually an acceptable convergence is obtained by using α value of 0.1 to 0.2, but the selection of most appropriate value for a special case depends on the conditions of the problem. In addition to the mentioned studies, the *UDT* has been studied in many other works which demonstrate different applications of this theory and its efficiency in designing more proper seismic resistant structures. Several examples are the studies conducted by Moghadam *et al.* (2005), Moghadam and Karami Mohammadi (2006), Moghadam and Hajirasouliha (2004, 2005, 2006a, b), Hajirasouliha and Moghadam (2009), Moghadam (2009) and Hajirasouliha *et al.* (2011).

2.2 Description of models

In the present study, three EBFs (as shown in Fig. 1) with 3, 5 and 10 stories have been considered. The height of the story and the span length for these buildings are selected to be 3.96 m and 9.14 m (13 ft and 30 ft), respectively. Also, the length of the link-beam is considered to be

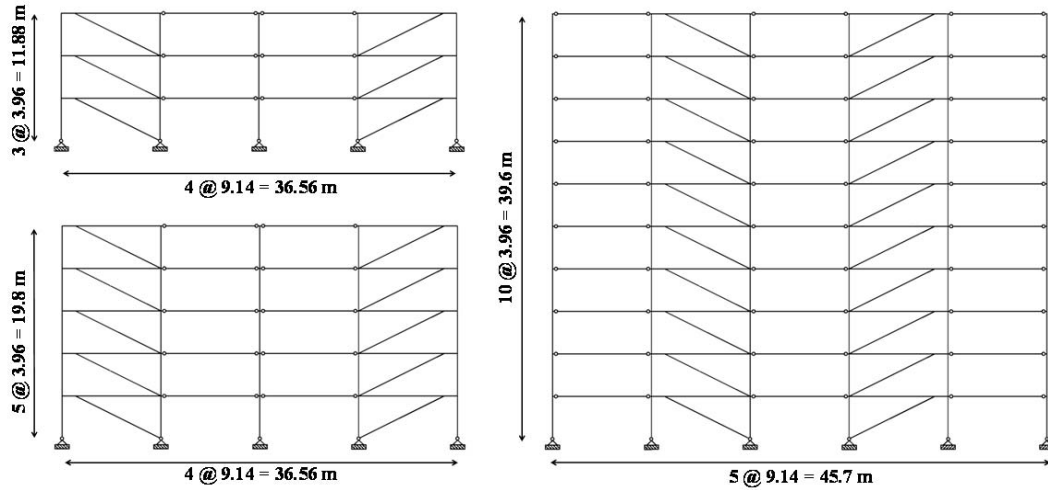


Fig. 1 Typical geometry of considered eccentrically braced frames

1.22 m (4 ft) in all stories.

A set of twelve far-field ground motion records are used for input excitation as listed in Table 1. These excitations are selected from ATC-63 (2007) and all correspond to sites of soil profile similar to type D of ASCE/SEI 7-10. The ground motions are scaled such that the spectral acceleration of each record matches the spectral acceleration of the design spectrum at the fundamental period of the structure that is being analyzed. The comparison of ASCE/SEI 7-10 design spectrum ($S_s = 2.3$ g, $S_1 = 0.84$ g) with the average of 12 selected earthquakes are shown in Fig. 2 and the parameters of seismic design of the frames are summarized in Table 2.

Table 1 Strong ground motion characteristics

No.	Mag.	Year	Event	Fault type	Station name	PGA (g)
1	6.7	1994	Northridge	Blind thrust	Beverly Hills-14145 Mulhol	0.52
2	6.7	1994	Northridge	Blind thrust	Canyon Country-W Lost Cany	0.48
3	7.1	1999	Duzce, Turkey	Strike-slip	Bolu	0.82
4	6.5	1979	Imperial Valley	Strike-slip	Delta	0.35
5	6.5	1979	Imperial Valley	Strike-slip	El Centro Array #11	0.38
6	6.9	1995	Kobe, Japan	Strike-slip	Shin-Osaka	0.24
7	7.5	1999	Kocaeli, Turkey	Strike-slip	Duzce	0.36
8	7.3	1992	Landers	Strike-slip	Yermo Fire Station	0.22
9	7.3	1992	Landers	Strike-slip	Coolwater	0.24
10	6.9	1989	Loma Prieta	Strike-slip	Capitola	0.53
11	6.9	1989	Loma Prieta	Strike-slip	Gilroy Array #3	0.56
12	6.5	1987	Superstition Hills	Strike-slip	El Centro Imp. Co. Cent	0.36

Table 2 Parameters for seismic design of the EBF frames

Parameters	3-story	5-story	10-story
S_s	2.380 g	2.380 g	2.380 g
S_1	0.840 g	0.840 g	0.840 g
F_a	1.000	1.000	1.000
F_v	1.500	1.500	1.500
S_{Ds}	1.587 g	1.587 g	1.587 g
S_{D1}	0.840 g	0.840 g	0.840 g
Site class	D	D	D
Seismic use group	I	I	I
Seismic design category	E	E	E
Building height	39 ft	65 ft	130 ft
Importance factor	1.00	1.00	1.00
T	0.46	0.68	1.15
R	8	8	8
C_s	0.1975	0.1544	0.0913
W	4630 kips	7660 kips	15700 kips
V	914.425 kips	1182.704 kips	1433.41 kips

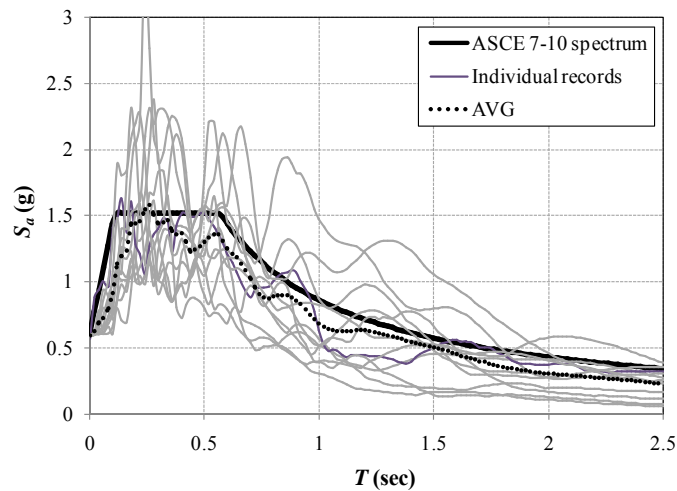
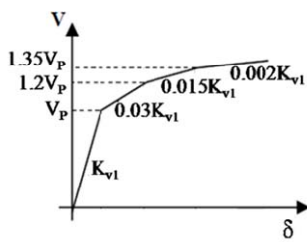


Fig. 2 A comparison of ASCE/SEI 7-10 design spectrum ($S_s = 2.3$ g, $S_1 = 0.84$ g) with the average of 12 selected earthquakes

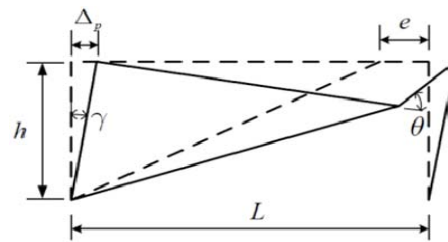
For the nonlinear dynamic analyses, the 2-dimensional (2D) analytical model of the EBFs is developed using the computer program *Open System for Earthquake Engineering Simulation* (OpenSees). The stress-strain behaviour of steel was modeled with “Hysteretic Material” in OpenSees. Beams and columns are both modeled using nonlinear Beam-column elements with

fiber sections. Spread plasticity models are employed to model nonlinear behaviour of beam and column elements. In this model, the plastic length is updated at each step of the analysis as a function of the instantaneous moment diagram in the element. It is useful to note that OpenSees does not have an explicit buckling model for steel braces. To include buckling of braces in the simulation, these elements are modeled with a maximum initial imperfection of $L/1000$ (out-of-straightness at mid-length).

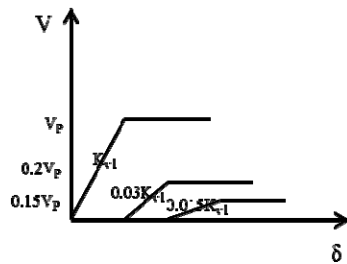
According to Rozon *et al.* (2008) and Richards and Uang (2006), the link-beams are modeled using an elastic beam element (Fig. 3(d)). Three translational springs operate in parallel at each end of the beam element in order to achieve a multilinear force deformation relationship using bilinear spring elements. The behaviour of each spring, represented by a bilinear force-deformation curve in Fig. 3(c). Individual spring properties were calculated such that the combined force-deformation relationships of the springs at either end correspond to those indicated in Fig. 3a. In Fig. 3(a) link shear, V , is plotted against the distance between the internal and external nodes. In Table 3, there are properties for plotting Fig. 3(a) and the V is based on nominal resistance ($V_p = 0.55 \phi A_y R_y F_y$, with $\phi R_y = 1.0$).



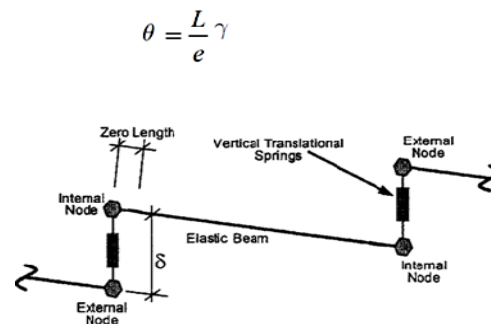
(a) Properties of the link-beams



(b) Shear deformation in the link-beams, θ



(c) Bilinear force deformation curve of the each springs



(d) Schematic of link-beams

Fig. 3 Modeling of the link-beams

Table 3 Properties of link-beam for plotting Fig. 3(a)

V_1/V_p	k_{v1}	V_2/V_p	k_{v2}	V_3/V_p	k_{v3}	k_{v4}
1.00	$2 GA_w/e$	1.20	$0.03 k_{v1}$	1.35	$0.015 k_{v1}$	$0.02 k_{v1}$

2.3 Application of optimization algorithm

As discussed before, the optimum performance of a structure during the given earthquake can be achieved based on the concept of uniform distribution of deformation. Also, it was described that the application of this concept will result in an optimum distribution of material in the structure. In this part, it is intended to use an optimization algorithm in order to locate the most efficient design in terms of structural weight and seismic performance. The objective of this optimization process is to minimize structural weight while satisfying the life safety (LS) performance level according to ASCE 41-06 (2007). For this purpose, maximum displacements, maximum rotation of plastic hinges, and maximum capacity of force controlled elements are considered as optimization constraints.

Different structural parameters can be regarded as design variables in the optimization procedures. Since the seismic behaviour of an EBF system is mostly governed by properties of the link-beams, the web shear area of these elements (which is in direct proportion to shear deformation of the link-beam) is considered as the major design variable in the present study. Other properties of the link-beams can be determined once their cross sectional area becomes known as it will be discussed later. Also, properties of other structural elements can be determined based on the obtained properties for the link-beams. In accordance with the concept of *UDT*, the optimization algorithm consists of the following steps:

- (1) An initial structure is designed to meet the requirements of the ANSI/AISC 360-10. The gravity and seismic loads are determined in accordance with ASCE/SEI 7-10.
- (2) The frame is subjected to the excitation and maximum shear deformation of the link-beams is calculated through nonlinear dynamic analysis.
- (3) Based on the concept of *UDT*, the cross sectional area of web should be increased in the link-beams with shear deformation, θ , greater than the target shear deformation, θ_t , and should be decreased in the link-beams where θ is less than θ_t . To achieve this, the following equation is used in this study

$$(A_w)_{i+1} = (A_w)_i \left[\frac{\theta}{\theta_t} \right]^\alpha \quad (2)$$

Where $(A_w)_i$ is the link-beam web shear area at i^{th} iteration, $(A_w)_{i+1}$ is the modified value of link-beam web shear area and α is the convergence coefficient. In this study, an acceptable convergence has been obtained for a value of α equal to 0.1. Also, the target shear deformation of the link-beams, θ_t , is considered to be equal to 0.11 (rad), a value associated with the life safety (LS) performance level according to ASCE 41-06. The graphical definition of the parameter θ is given in Fig. 3(b).

It should be noticed that for some ground motions, achieving the target shear deformation in the link-beams, $\theta_t = 0.11$ (rad), may need further weakening of the structural members and cause violation of design constraints. In these cases, the parameter θ_t is assumed to be 0.11 (rad) at the beginning but its value is updated during the optimization process using bellow equation

$$\theta_t = \min\{0.11 \text{ (rad)}, \max(\theta)\} \quad (3)$$

- (4) After modification of the link-beams, other frame members are sized to satisfy below equation

$$\lambda = \lambda_i \quad (4)$$

$$\lambda = \begin{cases} \left(\frac{P_r}{\phi P_n} \right) + \frac{8}{9} \left(\frac{M_r}{\phi M_n} \right) & \left(\frac{P_r}{\phi P_n} \right) \geq 0.2 \\ \left(\frac{P_r}{\phi P_n} \right) + \left(\frac{M_r}{\phi M_n} \right) & \left(\frac{P_r}{\phi P_n} \right) < 0.2 \end{cases} \quad (5)$$

Where, the parameter λ_i is assumed to be 0.9 for low-rise and 0.8 for high-rise buildings. In Eq. (5), P_r and M_r are the maximum axial force and bending moment due to gravity and lateral loads, P_n and M_n are the nominal axial and bending capacities and ϕ is the resistance factor which should be taken as 0.9 for both axial and bending capacities. In order to satisfy Eq. (4), the plastic modulus of each element is repeatedly modified using below equation

$$Z_{j+1} = Z_j \left[\frac{\lambda}{\lambda_i} \right]^\alpha \quad (6)$$

Where Z_j is the plastic modulus of an element at j^{th} sub-iteration and Z_{j+1} is the modified value of plastic modulus for that element.

- (5) The modified frame is reanalyzed using the selected excitations and maximum shear deformation of the link-beams is calculated. Theoretically, as the structure approaches to the state of uniform deformation, the coefficient of variation of maximum shear deformation in the link-beams, cov_θ , should tend to zero. In practice, if the cov_θ is considered to be small enough, we can stop and consider the pattern as practically optimum. Otherwise the analysis continues from step 3.

3. Performance of optimized EBFs

As it was mentioned before, the objective of optimization in this study is to minimize structural weight of EBFs by uniform distribution of shear deformation in link-beams. Fig. 4 illustrates the variation of design variables for 3-story EBF from first feasible answer toward the final answer. This figure has been obtained for the first ground motion record in Table 1. The coefficient of variation of shear deformation in link-beams, cov_θ , is displayed in Fig. 4(a) which indicates a reduction from 0.27 to 0.06 during optimization process. Also, the ratio of structural weight to the optimum weight, (W/W_{opt}) is displayed in Fig. 4(b). As it is clear from Fig. 4, the reduction in cov_θ is generally accompanied by a reduction in structural weight of EBF, which is in agreement with the concept of *UDT*.

Fig. 5 displays cov_θ at the final step of optimization for 3, 5 and 10 story EBFs subjected to 12 earthquake records of Table 1. As it can be seen from this figure, for most of 3 and 5 story EBFs the final value of cov_θ is less than 10%. For two 5-story and eight 10-story EBFs this parameter is between 10% and 20%. For these models it was not possible to achieve a smaller value for cov_θ because of design constraints and finite number of considered section profiles. However, the resultant EBFs are the more efficient ones between all possible structures.

Fig. 6 displays the inter-story drift distribution for near optimum design models subjected to the selected ground motion records. Although these structures are optimized by uniform distribution

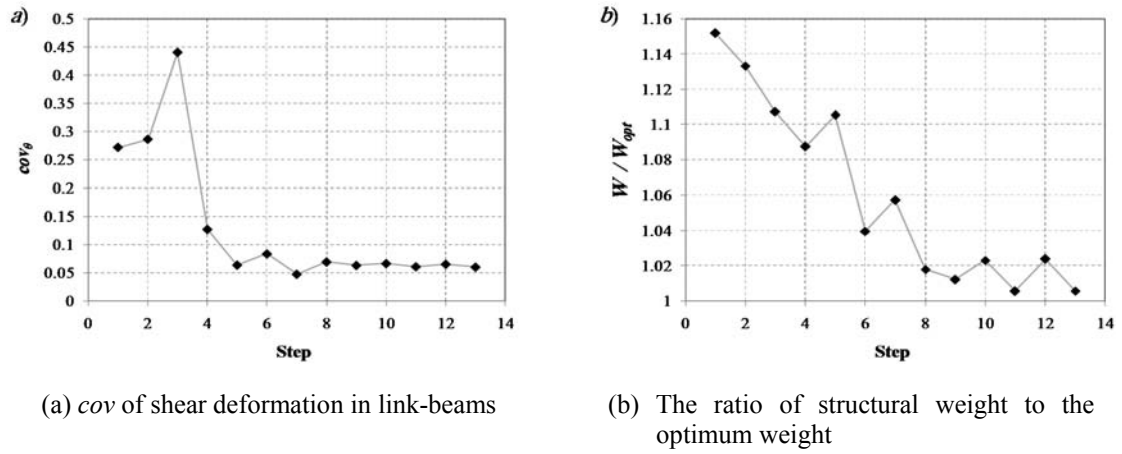


Fig. 4 Optimization of design variables in 3-story EBF

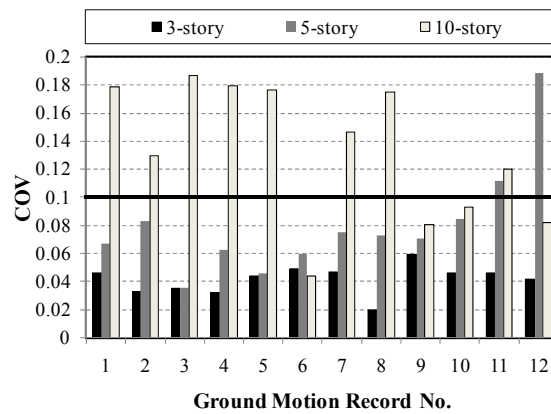


Fig. 5 Final value of cov_{θ} for optimized EBFs

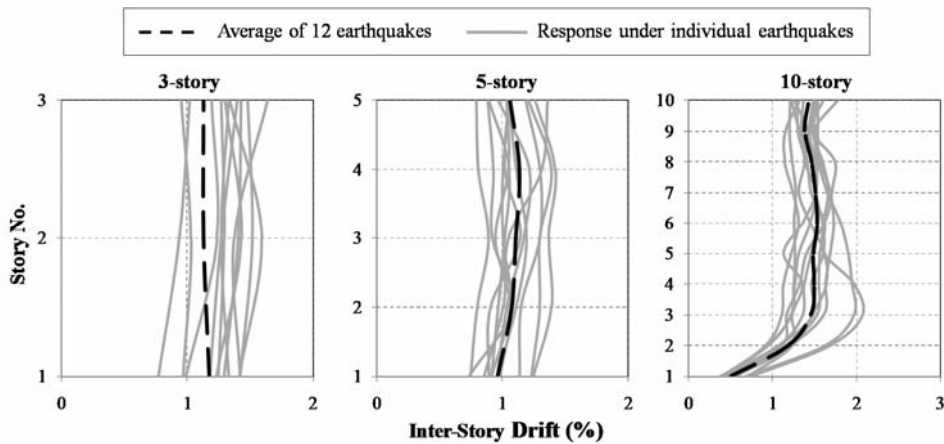


Fig. 6 Inter-story drift of optimized EBFs subjected to earthquake records of Table 1

of shear deformation in the link-beams, but as it is apparent from Fig. 6 their inter-story drift have become almost uniform too. In Fig. 7, sections of a sample EBF that subjected to the first ground motion of Table 1, can be seen before and after optimization.

4. Comparison with existing load patterns

4.1 Selected load patterns

As the preliminary design of most buildings is based on equivalent static forces, the optimization method used in this study needs to be compared against these conventional load patterns. In this section, a set of nonlinear dynamic analyses is carried out to investigate the efficiency of *UDT* against such loading patterns. The selected load patterns and their suggested way for distributing equivalent static forces are as follows:

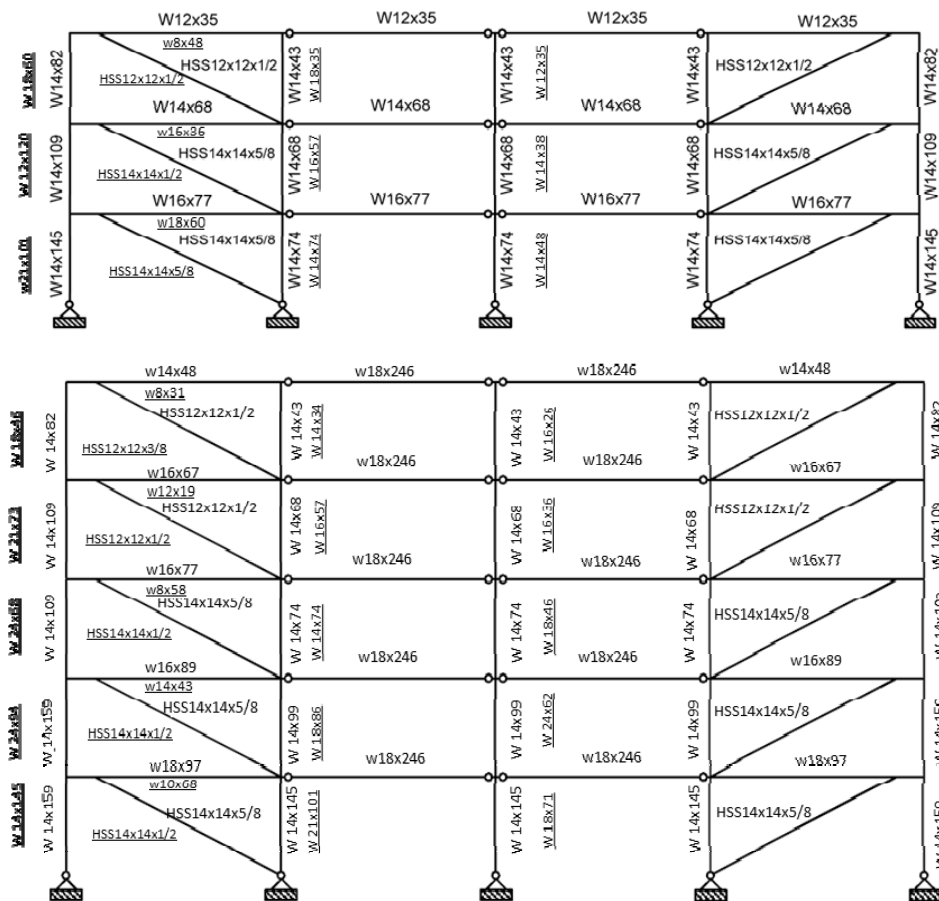


Fig. 7 Sections of an EBF subjected to the first ground motion of Table 1, before and after optimization (Note: Sections obtained from optimization process have shown with lines under them)

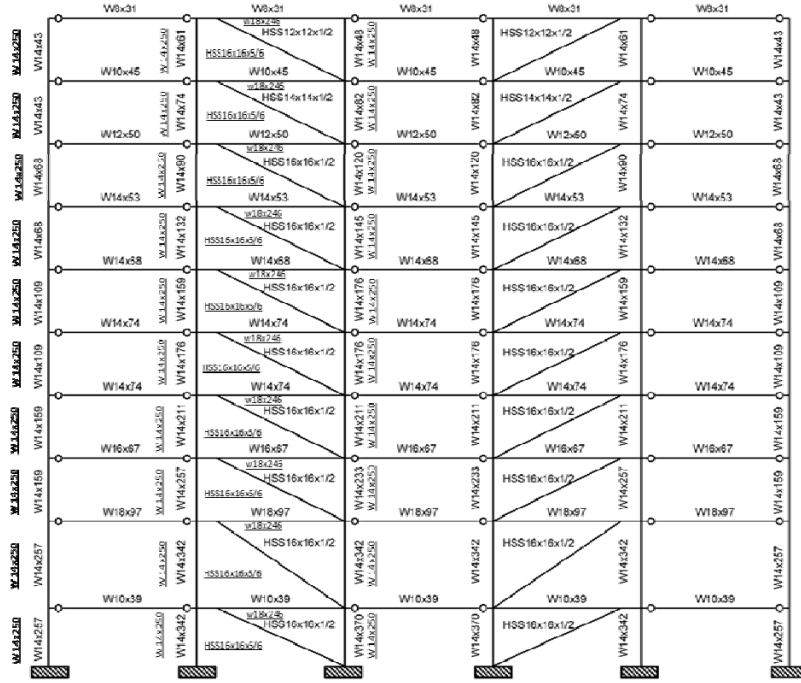


Fig. 7 Continued

- (1) **Load pattern of ASCE/SEI 7-10:** According to the ASCE/SEI 7-10 load pattern, the calculated base shear, V , shall be distributed within the stories using

$$F_i = \frac{w_i h_i^k}{\sum_{j=1}^n w_j h_j^k} V \quad i = 1, 2, 3, \dots, n \quad (7)$$

where

$$k = \begin{cases} 1 & \text{if } T \leq 0.5 \\ \min\{0.5T + 0.75, 2\} & \text{if } 0.5 < T < 2.5 \\ 2 & \text{if } T \geq 2.5 \end{cases} \quad (8)$$

In above equations, F_i is the lateral force at level i , w_i and h_i are the weight and height of the i^{th} floor above the base, n is the number of stories and T is the fundamental period of building.

- (2) **Load pattern suggested by Karami Mohammadi et al. (2004):** This distribution is indeed a rectangular pattern accompanied by a concentrated force at the top floor, F_t . Using this pattern, the lateral force at each level, F_i , can be obtained as

$$F_i = \frac{(V - F_t)}{n} \quad i = 1, 2, 3, \dots, n \quad (9)$$

$$F_i = \alpha TV \quad (10)$$

Where, V is the total base shear calculated by equating $\sum_{i=1}^n F_i$ from Eq. (7) and Eq. (9). The coefficient α is a function of fundamental period, T , and target ductility, μ , as follows

$$\alpha = (0.9 - 0.04\mu) \times e^{-(0.6+0.03\mu)T} \quad (11)$$

In this study, the target ductility is assumed to be $\mu = 4$ when the equation suggested by Karami Mohammadi *et al.* (2004) is used as the lateral load pattern.

- (3) **Load pattern suggested by Chao and Goel (2007):** This load pattern is based on the study of inelastic responses of various types of structural systems, using extensive nonlinear dynamic analysis results. The suggested expression is as follows

$$F_i = C'_{vi} V \quad i = 1, 2, 3, \dots, n \quad (12)$$

Where, V is the design base shear calculated according to Chao and Goel (2005) and

$$C'_{vi} V = (\beta_i - \beta_{i+1}) \left(w_n h_n / \sum_{j=1}^n w_j h_j \right)^{\alpha T^{-0.2}} \quad \text{when } i = n \Rightarrow \beta_{i+1} = 0 \quad (13)$$

$$\beta_i = \left(\sum_{j=1}^n w_j h_j / w_n h_n \right)^{\alpha T^{-0.2}} \quad (14)$$

Where, β_i is the shear distribution factor at level i and other parameters are defined before. The value of parameter α was originally proposed as 0.5 by Lee and Goel (2001), which was later revised to be 0.75 based on more extensive nonlinear dynamic analyses on eccentrically braced frames (EBFs) and special truss moment frames (STMFs) by Chao and Goel (2007).

- (4) **Load pattern suggested by Deguchi *et al.* (2008):** Providers of this load pattern claim that its application avoids the concentration of deformation and damage in just one story and makes each story deformation and damage uniform over the height of the structure. According to this load pattern, the story strength is described as

$$F_i = C_i W_i = C_i \alpha_i W \quad i = 1, 2, 3, \dots, n \quad (15)$$

Where, W_i is the weight above the level i (defined by $\sum_{j=i}^n w_j$), W is the total weight of the structure and α_i is the dimensionless height defined as

$$\alpha_i = \frac{h_n - h_i}{h_n} \quad (16)$$

Where h_n is the total height of the structure and h_i is the height of the i^{th} floor above the base. In Eq. (15), the parameter C_i is called the shear coefficient which specifies the intensity and vertical distribution of the seismic load

$$C_i = C_B A_i \quad (17)$$

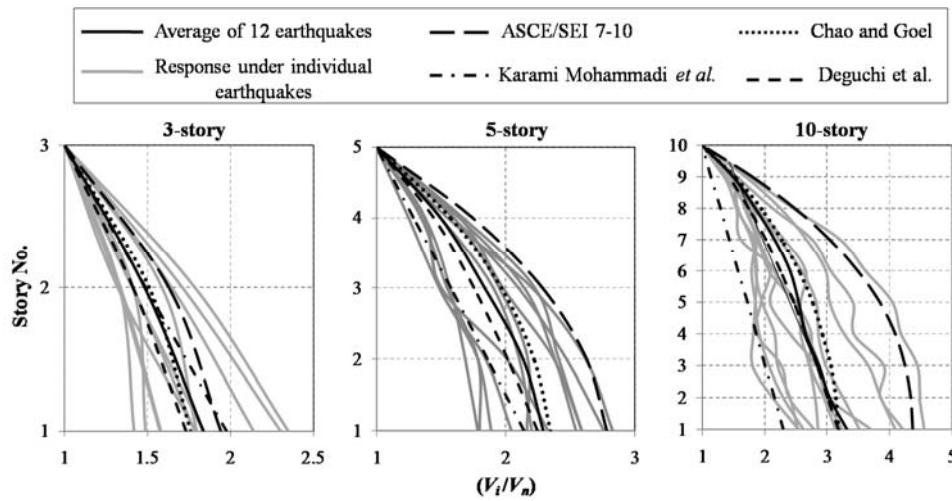


Fig. 8 Shear strength distribution of optimized EBFs and selected load patterns

Where, C_B is the base shear coefficient (which in this study is calculated according to which in this study is calculated according to ASCE/SEI 7-10) and A_i is the shear coefficient distribution defined as $(1/\sqrt{\alpha_i})$.

4.2 Comparison of shear strength distributions

As the shear strength of each story is in proportion to the weight of that story, the distribution of shear strength over the height of the structure can be treated as an optimization parameter. For 3, 5 and 10 story EBFs, the optimum shear strength distribution patterns corresponding to the selected excitations are determined, and plotted in Fig. 7. In this figure, V_i is the shear strength of the i^{th} story and V_n is the shear strength of the top story. Also for comparison purpose, the shear strength distribution corresponding to the prescribed loading patterns is calculated and plotted in Fig. 8.

As it can be seen from this figure, the optimum strength distribution pattern depends on the input ground motion and varies from record to record. A comparison between these optimum strength distributions and the one corresponding to the ASCE/SEI 7-10 load pattern shows that for nearly all excitations the optimum design requires less strength which means that the ASCE/SEI 7-10 load pattern is very conservative. Although for some of excitations the strength distribution patterns proposed by Chao and Goel (2007) and Deguchi *et al.* (2008) significantly deviate from the optimum strength distribution, but these two patterns are very close to the average of optimum strength distributions. Accordingly, it can be expected that these load patterns will generally lead to more uniform deformations of elements as well as stories over the height of the structure, which will be discussed in the next section.

4.3 Comparison of link-beams rotation

Recent design guidelines place limits on the acceptable values of response parameters,

implying that exceeding these limits is a violation of a performance objective. Among various response parameters of EBFs, the link-beam rotation is considered as a reliable damage index, and is widely used as a failure criterion. In this section, optimized and conventionally designed structures are compared in terms of link-beams rotation. For this purpose, the 10-story EBF is redesigned using four prescribed loading patterns and subjected to 12 selected ground motions. The design base shear for the load patterns of ASCE/SEI 7-10 and Deguchi *et al.* (2008) is computed as 6450 kN (1450 kips). For the load patterns proposed by Karami Mohammadi *et al.* (2004) and Chao and Goel (2007) the design base shear is calculated as 3127 kN (703 kips) and 5560 kN (1250 kips), respectively. Fig. 9 compares the link-beam rotation for selected load patterns and near optimum design model.

It is illustrated in Fig. 9 that for none of the considered load patterns, link-beam rotation demand is distributed uniformly. On the other hand, the maximum demand occurs almost at the second and third stories. Also it is shown that the application of *UDT* leads to a structure with a rather more uniform deformation of link-beams. As a result, these structures suffer less damage as compared with structures designed for other loading patterns.

According to Fig. 9, for all of the considered load patterns the rotation of the link-beam in some stories exceeds the rotation associated with the LS performance level according to ASCE 41-06 ($\theta_i = 0.11$ (rad)). Assuming that the probability distribution of rotation in link-beams under different

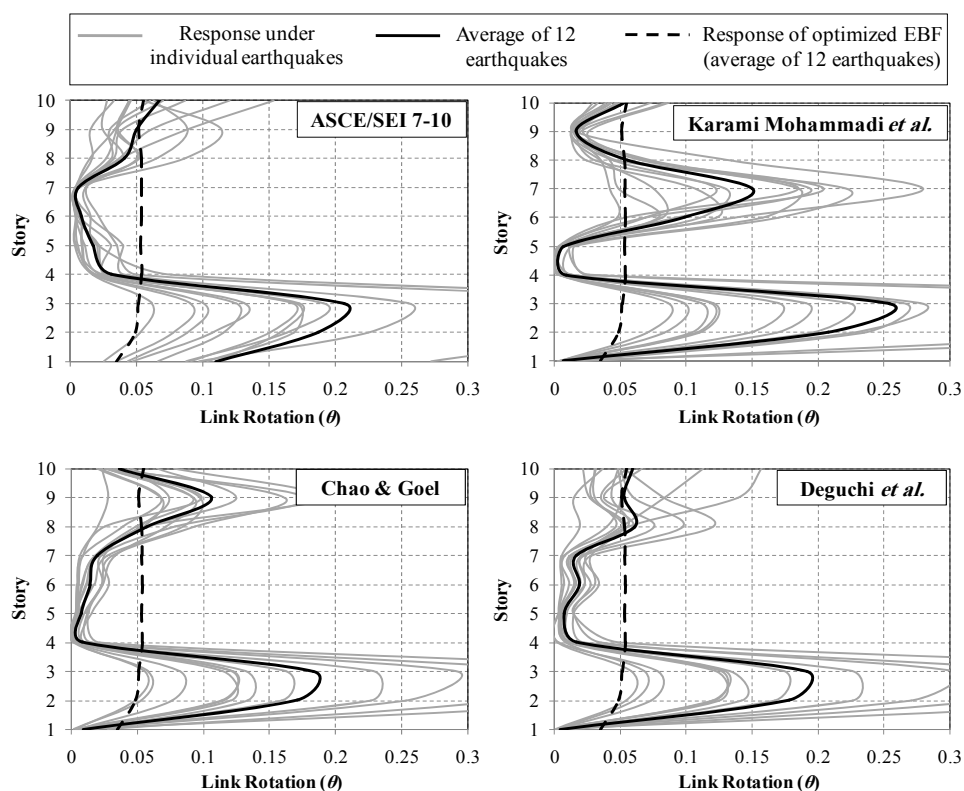


Fig. 9 Comparison of link-beams rotation for selected load patterns and near optimum design model

Table 4 Probability of violation from LS performance level in terms of link rotation (%)

Story	ACSE/SEI 7-10 (2010)	Karami Mohammadi <i>et al.</i> (2004)	Chao and Goel (2007)	Deguchi <i>et al.</i> (2008)
1	40.55	0.01	0.03	0.00
2	67.35	67.24	56.48	59.42
3	71.93	71.18	56.38	58.71
4	0.16	0.06	0.00	0.06
5	2.63	0.00	0.00	0.00
6	0.00	32.70	0.08	0.24
7	0.00	57.60	0.23	0.04
8	1.80	1.33	10.44	0.77
9	3.42	0.00	34.21	2.22
10	11.50	3.19	0.46	9.49
AVG	19.94	23.33	15.83	13.10

excitations follows a lognormal distribution, the probability of exceeding the link-beam rotation associated with the LS performance level is calculated for different load patterns and listed in Table 4. From previous section it was expected that the application of load patterns proposed by Chao and Goel (2007) and Deguchi *et al.* (2008) would result in a more efficient design. This can be seen also in Table 4, which shows that exceeding the LS performance level is less likely for EBFs designed based on these load patterns.

Generally, in traditional design method there are two possible solutions to improve seismic performance of the structures. The first solution is to change lateral load pattern of the seismic forces. Evaluation of four different load patterns in Fig. 9 revealed that this solution cannot be an efficient way while the rotation of link-beams in EBFs designed according to these load patterns violates from LS performance level criterion in some stories. Also it should be noted that changing the lateral load pattern will not necessarily improve seismic performance of the structure under all possible excitations. In other words, if a structure is designed using a special load pattern and its response is in a good state under a given seismic event, there is no guarantee that this structure will not violate from design criteria when subjected to another earthquake event.

The second way to improve seismic performance of a structure is to increase its design base shear. To see effect of this factor on the seismic performance of EBFs, the base shear of all considered load patterns is increased to 11120 kN (2500 kips) and the analyses are repeated. Probability of violation from LS performance level criterion ($\theta_l = 0.11$ (rad)) for EBFs designed with increased base shear is calculated for each load pattern and given in Table 5. As it can be seen from this table, the increase of design base shear in EBFs will decrease the probability of violation from the selected performance level criterion but even in these EBFs the value of link-beam rotation in some stories is more than the specified limiting link rotation. To meet the design requirements in the link-beams of all stories it may be needed to further increase the design base shear of the structure. This overestimation of base shear will lead to an uneconomical design which contains a lot of inefficient material in strong parts of the structure, e.g., 4th, 5th, 6th and 7th stories in Fig. 9.

Table 5 Probability of violation from LS performance level for EBFs designed with increased base shear (%)

Story	ACSE 7-10 (2010)	Karami Mohammadi <i>et al.</i> (2004)	Chao and Goel (2007)	Deguchi <i>et al.</i> (2008)
1	14.39	2.17	0.42	0.00
2	48.43	71.91	35.61	57.29
3	53.43	68.69	36.47	61.50
4	1.22	0.00	0.00	0.01
5	0.00	0.00	0.00	0.00
6	0.00	0.00	0.00	0.00
7	0.00	0.20	0.16	0.00
8	0.01	0.37	0.26	0.89
9	1.43	0.00	1.54	0.39
10	1.34	0.00	11.83	4.10
AVG	12.03	14.33	8.63	12.42

Above discussion indicates efficiency of *UDT* in optimizing seismic performance of eccentrically braced frames through changing both load pattern and design base shear to have a more proper structure with optimum distribution of strength (material) in all structural elements.

5. Conclusions

This paper presents a practical method for optimization of eccentrically braced steel frames, based on the concept of uniform deformation theory (*UDT*). This includes design of an initial structure according to conventional elastic design procedures, followed by an iterative assessment process using nonlinear dynamic analyses till the state of uniform deformation is achieved. It is shown in this paper that the application of *UDT* leads to a structure with a rather more uniform inter-story drift distribution. Although the EBFs considered in this paper had been optimized by uniform distribution of shear deformation in the link-beams, but their inter-story drift became almost uniform too. For further investigation, shear strength distribution pattern and link-beams rotation of optimized EBFs were compared to the same quantities corresponding to four existing load patterns. It is concluded that the optimized EBFs suffer less damage as compared with the structures designed for conventional load patterns. Finally, evaluation of considered load patterns revealed that the shear strength distribution patterns proposed by Chao and Goel (2007) and Deguchi *et al.* (2008) are very close to the average of optimum strength distributions and as a consequence, exceeding the LS performance level is less likely for EBFs designed based on these load patterns.

References

Anderson, J.C., Miranda, E., Berto, V.V. and Kajima Research Team (1991), *Evaluation of the Seismic Performance of Thirty-Story RC Building*, UCB/EERC 91/16, Berkeley, Earthquake Engineering

- Research Center, University of California, CA, USA.
- ANSI/AISC 360-10 (2010), *Specification for Structural Steel Buildings*, American Institute of Steel Construction (AISC), Chicago, IL, USA.
- ASCE/SEI 41-06 (2007), *Seismic Rehabilitation of Existing Building*, American Society of Civil Engineers (ASCE).
- ASCE/SEI 7-10 (2010), *Minimum Design Loads for Buildings and other Structures*, ASCE Standard, American Society of Civil Engineers (ASCE).
- ATC 63 (2007), *Quantification of Building System Performance and Response Parameters*, Prepared by Applied Technology Council (ATC), CA, USA.
- BCJ (1997), *BCJ Seismic Provisions for Design of Building Structures*, The Building Center of Japan (BCJ), Tokyo, Japan.
- Chao, S.H. and Goel, S.C. (2005), *Performance-Based Seismic Design of EBF using Target Drift and Yield Mechanism as Performance Criteria*, A report on research partly sponsored by the American Institute of Steel Construction (AISC), Department of Civil and Environmental Engineering, The University of Michigan, Ann Arbor, MI, USA.
- Chao, S.H. and Goel, S.C. (2007), "A seismic design lateral force distribution based on inelastic state of structures", *Earthquake Spectra*, **23**(3), 547-569.
- Chopra, A.K. (2001), *Dynamic of Structures: Theory and Applications to Earthquake Engineering*, (2nd Edition), Prentice Hall Inc., London, UK.
- Deguchi, Y., Kawashima, T., Yamanari, M. and Ogawa, K. (2008), "Seismic design load distribution in steel frame", *The 14th World Conference on Earthquake Engineering*, Beijing, China, October.
- Hajirasouliha, I. (2005), *The Effect of the Distribution of Seismic Resistant Factors on the Performance of Structure*, Ph.D. Dissertation, Civil Engineering Department, Sharif University of Technology, Tehrān, Iran.
- Hajirasouliha, I. and Moghadam, H., (2009), "New lateral force distribution for seismic design of structures", *J. Struct. Eng., ASCE*, **135**(8), 906-915.
- Hajirasouliha, I., Asadi, P. and Pilakoutas, P. (2011), "An efficient performance-based seismic design method for reinforced concrete frames", *Earthq. Eng. Struct. Dyn.*, **41**(4), 663-679.
- Hart, G.C. (2000), "Earthquake forces for the lateral force code", *Struct. Des. Tall Buil.*, **9**(1), 49-64.
- Karami Mohammadi, R. (2001), *Optimum Distribution of Dynamic Characteristics within the Structure to Reduce Seismic Damage*, Ph.D. Dissertation, Civil Engineering Department, Sharif University of Technology, Tehrān, Iran.
- Karami Mohammadi, R., El-Naggar, M.H. and Moghadam, H. (2004), "Optimum strength distribution for seismic resistant shear-buildings", *Int. J. Solids Struct.*, **41**(22-23), 6597-6612.
- Lee, S.S. and Goel, S.C. (2001), "Performance based seismic design of structures using target drift and yield mechanism", *US-Japan Seminar on Advanced stability and Seismicity Concept for Performance Based Design of Steel and Composite Structures*, Kyoto, Japan.
- Martinelli, L., Perotti, F. and Bozzi, A. (2000), "Seismic design and response of a 14-story concentrically braced steel building", *Behav. Steel Struct. Seismic Areas*, 327-355.
- Moghadam, H. (2009), "On the optimum performance-based design of structures", *Proceedings of a U.S.-Iran Seismic Workshop*, Irvine, CA, USA.
- Moghadam, H. and Hajirasouliha, I. (2004), "A new approach for optimum design of structures under dynamic excitation", *Asian J. Civil Eng. (Building and Housing)*, **5**(2), 69-84.
- Moghadam, H. and Hajirasouliha, I. (2005), "Fundamentals of optimum performance based design for dynamic excitation", *ScientiaIranica*, **12**(4), 368-378.
- Moghadam, H. and Hajirasouliha, I. (2006a), "Toward more rational criteria for determination of design earthquake forces", *Int. J. Solids Struct.*, **43**(9), 2631-2645.
- Moghadam, H. and Hajirasouliha, I. (2006b), "An investigation on accuracy of pushover analysis for estimating the seismic deformation of braced steel frames", *J. Construct. Steel Res.*, **62**(4), 343-351.
- Moghadam, H. and Karami Mohammadi, R. (2006), "More efficient seismic loading for multi degrees of freedom structures", *J. Struct. Eng., ASCE*, **132**(10), 1673-1677.

- Moghadam, H., Hajirasouliha, I. and Doostan, A. (2005), "Optimum seismic design of concentrically braced steel frames: Concepts and design procedures", *J. Construct. Steel Res.*, **61**(2), 151-166.
- Moghaddam, H., Hosseini Gelekolai, S.M., Hajirasouliha, I. and Tajali, F. (2012), "Evaluation of various proposed lateral load patterns for seismic design of steel moment resisting frames", *The 15th World Conference on Earthquake Engineering*, Lisbon, Portugal, September.
- OpenSees (Open System for Earthquake Engineering Simulation), Mazzoni, S., McKenna, F. and Fenves, G.L. (Version 2.2.2), UC Berkeley, CA, USA. <http://opensees.berkeley.edu>
- Park, K. and Medina, R.A. (2006), "Lateral load patterns for conceptual seismic design of frames exposed to near-fault ground motions", *Proceedings of the 8th U.S. National Conference on Earthquake Engineering*, Paper No. 949, San Francisco, CA, USA.
- Richards, P.W. and Uang, C.M. (2006), "Testing protocol for short links in eccentrically braced frames", *J. Struct. Eng.*, **132**(8), 1183-1191.
- Rozon, J., Koboovic, S. and Tremblay, R. (2008), "Study of global behaviour of eccentrically braced frames in response to seismic loads", *The 14th World Conference on Earthquake Engineering*, Beijing, China, October.
- UBC (1997), *Structural Engineering Design Provisions, Uniform Building Code*, International Conference of Building Officials, Vol. 2.

BU